

DECONVOLUTION OF POISSONIAN IMAGES WITH THE PURE-LET APPROACH

Jizhou Li¹, Florian Luisier² and Thierry Blu¹

¹ Department of Electronic Engineering, The Chinese University of Hong Kong, Hong Kong

² Roche Diagnostics Hematology, Boston, MA

ABSTRACT

We propose a non-iterative image deconvolution algorithm for data corrupted by Poisson noise. Many applications involve such a problem, ranging from astronomical to biological imaging. We parametrize the deconvolution process as a linear combination of elementary functions, termed as linear expansion of thresholds (LET). This parametrization is then optimized by minimizing a robust estimate of the mean squared error, the “Poisson unbiased risk estimate (PURE)”. Each elementary function consists of a Wiener filtering followed by a pointwise thresholding of undecimated Haar wavelet coefficients. In contrast to existing approaches, the proposed algorithm merely amounts to solving a linear system of equations which has a fast and exact solution. Simulation experiments over various noise levels indicate that the proposed method outperforms current state-of-the-art techniques, in terms of both restoration quality and computational time.

Index Terms— Image deconvolution, Poisson noise, unbiased risk estimate, MSE estimation.

1. INTRODUCTION

Images are often corrupted by noise and blurring during the acquisition process. In a variety of applications, ranging from astronomical imaging to biological microscopy, the predominant source of noise follows a Poisson distribution due to the quantum nature of the photon-counting process at the detectors [1–5]. There are many efficient image restoration algorithms designed under an additive (often white) Gaussian noise assumption [6–10]. However, these approaches become sub-optimal for Poissonian images due to the signal-dependent nature of Poisson noise; i.e., the noise variance in each pixel is proportional to the intensity of the underlying signal. The development of deconvolution algorithms specifically designed for Poisson noise then becomes essential.

A popular method for Poissonian image deconvolution problems is the Richardson-Lucy (RL) algorithm [11, 12]. Regularized variants of the RL algorithm include total-variation [13, 14] and wavelet-based regularization [15, 16]. Additional approaches can be found in [2] and [17]. Most of these methods convert the deconvolution problem into the optimization of an objective function consisting of a data term, which quantifies the proximity between the estimated image and the measurement, plus a convex non-smooth regularizer (e.g., the log-likelihood [18, 19]). However, the Poisson log-likelihood is generally non-quadratic and non-separable, which often requires the application of relatively sophisticated optimization theory [20]. Other approaches bypass the Poisson statistical model in

favor of an additive Gaussian noise model through the Anscombe variance-stabilizing transform [21]. However, such approximations are inaccurate when the observed number of photons is small [22, 23] and are not really suited to deconvolution.

The major contribution of this paper is to extend the SURE deconvolution approach introduced in [10] to the Poisson noise case. We parametrize the deconvolution process as a linear combination of elementary functions, termed as linear expansion of thresholds (LET) [4, 10, 24]. Each elementary function then consists of a Wiener filtering followed by wavelet-domain thresholding. We finally use the Poisson unbiased risk estimate (PURE) to optimize these LETs that are adapted to the signal-dependent noise variance. Note that this optimization step is performed in the image-domain to ensure the global mean squared error (MSE) optimality [24, 25]. Importantly, in contrast to existing techniques, the proposed method is non-iterative; the PURE being quadratic in nature, the algorithm amounts to solving a linear system of equations, which is fast and has an exact solution.

This paper is organized as follows. We firstly introduce the theoretical basis of this work, specifically the PURE for deconvolution problem. Then we present our PURE-LET algorithm and provide a typical structure of the elementary function. Finally, we compare the proposed method with three state-of-the-art techniques over various noise levels.

2. THEORETICAL BACKGROUND

2.1. Problem statement

The observation model for a linear degradation caused by blurring and Poisson noise is given by

$$y = \alpha \mathcal{P} \left(\frac{\mathbf{H}\mathbf{x}}{\alpha} \right) \quad (1)$$

where $y \in \mathbb{R}^N$ denotes the distorted observation of the unknown true image $\mathbf{x} \in \mathbb{R}_+^N$, $\mathbf{H} : \mathbb{R}_+^N \rightarrow \mathbb{R}^N$ implements a convolution of the point spread function (PSF) h , $\mathcal{P}(\cdot)$ represents the effect of Poisson noise and $\alpha \in \mathbb{R}_+$ is the scaling factor, which controls the strength of noise. Specifically, larger values of α will lead to lower intensity images and thus higher Poisson noise.

Our objective is to find a function $\mathbf{F} : \mathbb{R}^N \rightarrow \mathbb{R}^N$ for the measured y such that $\hat{\mathbf{x}} = \mathbf{F}(y)$ is the closest possible to \mathbf{x} in the MSE sense. That is, ideally we would like to minimize

$$\text{MSE} = \frac{1}{N} \mathbb{E}\{\|\hat{\mathbf{x}} - \mathbf{x}\|^2\} = \frac{1}{N} \mathbb{E}\left\{ \sum_{n=1}^N (\hat{x}_n - x_n)^2 \right\}$$

where $\mathbb{E}\{\cdot\}$ denotes the mathematical expectation operator. Note that we intend to estimate the function \mathbf{F} instead of $\hat{\mathbf{x}}$ itself.

This work was supported by grants from the Research Grants Council (RGC) of Hong Kong (AoE/M-05/12). The authors would like to thank Christopher Gilliam for his careful reading of the manuscript.

2.2. Poisson unbiased risk estimate (PURE)

Since in practice we do not have access to the oracle MSE between \mathbf{x} and the estimate $\hat{\mathbf{x}}$, we will use an unbiased estimate of its expected value, which solely depends on the observed image y .

The expectation of the MSE between a given estimate $\hat{\mathbf{x}} = \mathbf{F}(y)$ and \mathbf{x} can be accurately computed from the observed image y by PURE using the following theorem:

Theorem 1 *Let $\mathbf{F}(y) = [f_n(y)]_{n=1\dots N}$ be an N -dimensional real-valued vector function. Considering the linear degradation model (1) and assuming \mathbf{H} is invertible, then the random variable (referred to as PURE)*

$$\epsilon = \frac{1}{N} \|\mathbf{F}(y)\|^2 - \frac{2}{N} \text{dif}_{\mathbf{H}} \mathbf{F}(y) + \frac{1}{N} \|\mathbf{x}\|^2 \quad (2)$$

is an unbiased estimate of the expected MSE; i.e.,

$$\mathbb{E}\{\epsilon\} = \frac{1}{N} \mathbb{E} \{ \|\mathbf{F}(y) - \mathbf{x}\|^2 \}$$

where $\text{dif}_{\mathbf{H}} \mathbf{F}(y) = \sum_{n=1}^N y_n \tilde{f}_n(y - \alpha e_n)$ and $\tilde{\mathbf{F}}(y) = \mathbf{H}^{-\text{T}} \mathbf{F}(y)$, e_n is the N -dimensional vector with components δ_{k-n} , $k = 1, 2, \dots, N$, $\mathbf{H}^{-\text{T}}$ is the inverse and transpose of \mathbf{H} .

This theorem is a natural extension of PURE in [4] to the distortion model (1). The unbiasedness between PURE and MSE indicates ϵ could be used as a reliable substitute of MSE for large N . Importantly, the last term $\|\mathbf{x}\|^2$ is irrelevant when minimizing ϵ , and all the other terms are computable in practice.

Considering the possible ill-posedness of the matrix \mathbf{H} , the Tikhonov-regularized inverse [2, 10] is used to approximate \mathbf{H}^{-1} :

$$\mathbf{H}_{\beta}^{-1} = \left(\mathbf{H}^{\text{T}} \mathbf{H} + \beta \mathbf{P}^{\text{T}} \mathbf{P} \right)^{-1} \mathbf{H}^{\text{T}}$$

for some parameter $\beta > 0$ and matrix $\mathbf{P} \in \mathbb{R}^N \times \mathbb{R}^N$. In this work, we choose \mathbf{P} as the discrete Laplacian operator and set $\beta = 1 \times 10^{-5} \alpha \mu$, where $\mu = \mathbb{E}\{y\}$ is the expected value of y . Thus the PURE in (2), without the constant $\|\mathbf{x}\|^2$, becomes:

$$\epsilon_{\beta} = \frac{1}{N} \|\mathbf{F}(y)\|^2 - \frac{2}{N} \text{dif}_{\mathbf{H}_{\beta}} \mathbf{F}(y) \quad (3)$$

Furthermore, a direct evaluation of $\text{dif}_{\mathbf{H}_{\beta}} \mathbf{F}(y)$ would require the calculation of $y^{\text{T}} \mathbf{H}_{\beta}^{-\text{T}} \mathbf{F}$ for N perturbed versions of the input y : $(y - \alpha e_n)$ for $n = 1, \dots, N$. Such an evaluation would be computationally unrealistic even with images of reasonable size (e.g. 256×256). Instead, we use the 1st-order derivative to approximate $\text{dif}_{\mathbf{H}_{\beta}} \mathbf{F}(y)$ given by:

$$\text{dif}_{\mathbf{H}_{\beta}} \mathbf{F}(y) \simeq y^{\text{T}} \mathbf{H}_{\beta}^{-\text{T}} (\mathbf{F}(y) - \alpha \partial \mathbf{F}(y))$$

where $\partial \mathbf{F}(y) = [\frac{\partial f_n(y)}{\partial y_n}]_{n=1, \dots, N}$ is the $N \times 1$ vector made of the first derivative of each function f_n with respect to y_n . Consequently, the PURE unbiased MSE estimate defined in (3) is well approximated by

$$\tilde{\epsilon} = \frac{1}{N} \|\mathbf{F}(y)\|^2 - \frac{2}{N} y^{\text{T}} \mathbf{H}_{\beta}^{-\text{T}} \mathbf{F}(y) + \frac{2\alpha}{N} y^{\text{T}} \mathbf{H}_{\beta}^{-\text{T}} \partial \mathbf{F}(y) \quad (4)$$

Note that, if \mathbf{F} is linear, the two MSE estimate, (3) and (4), are equivalent.

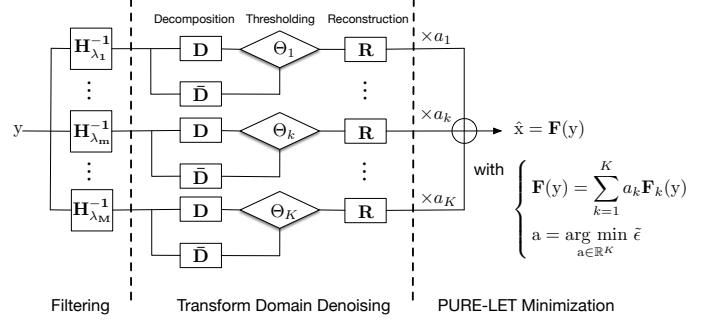


Fig. 1. Principle of the proposed PURE-LET approach.

3. MULTI-WIENER PURE-LET DECONVOLUTION

3.1. The PURE-LET approach

In order to find the function \mathbf{F} such that $\mathbf{F}(y)$ is close to \mathbf{x} , we describe the deconvolution process \mathbf{F} as a linear combination of K possibly non-linear element function \mathbf{F}_k , termed as linear expansion of thresholds (LET) [4, 10, 24]:

$$\mathbf{F}(y) = \sum_{k=1}^K a_k \mathbf{F}_k(y) \quad (5)$$

where $K \ll N$ is the number of linear coefficients $\mathbf{a} = [a_k]_{k \in [1, \dots, K]}$ of the LETs.

Accordingly, the deconvolution problem is reduced to finding the linear coefficients a_k by minimizing the MSE estimate $\tilde{\epsilon}$ defined in (4). By substituting (5) into (4) and performing differentiation over a_k , this minimization is equivalent to solving the following linear system of equations:

$$\sum_{k'=1}^K \mathbf{F}_k(y)^{\text{T}} \mathbf{F}_{k'}(y) a_{k'} = \underbrace{y^{\text{T}} \mathbf{H}_{\beta}^{-\text{T}} (\mathbf{F}_k(y) - \alpha \partial \mathbf{F}_k(y))}_{c_k} \quad (6)$$

for $k = 1, 2, \dots, K$. These equations could be summarized as $\mathbf{M}\mathbf{a} = \mathbf{c}$, where $\mathbf{M} = \mathbf{F}^{\text{T}} \mathbf{F} \in \mathbb{R}^{K \times K}$ and $\mathbf{c} = [c_1, \dots, c_K]^{\text{T}} \in \mathbb{R}^K$.

3.2. Construction of elementary function: multi-Wiener filtering followed by transform-domain thresholding

The elementary functions \mathbf{F}_k 's consist of multi-Wiener filtering followed by transform-domain thresholding. An illustrative description of the proposed deconvolution approach is shown in Fig. 1. The matrices $\mathbf{H}_{\lambda_k}^{-1} = (\mathbf{H}^{\text{T}} \mathbf{H} + \lambda_k \mathbf{P}^{\text{T}} \mathbf{P})^{-1} \mathbf{H}^{\text{T}}$ represent the Wiener filter with a given regularization parameter λ_k . $\mathbf{D} = [d_{i,j}]_{(i,j) \in [1, \dots, L] \times [1, \dots, N]}$ and $\mathbf{R} = [r_{i,j}]_{(i,j) \in [1, \dots, L] \times [1, \dots, N]}$ represent a pair of linear decomposition and reconstruction transforms that satisfies the perfect reconstruction condition $\mathbf{R}\mathbf{D} = \mathbf{I}$. A linear transformation $\tilde{\mathbf{D}} = [\tilde{d}_{i,j}]_{(i,j) \in [1, \dots, L] \times [1, \dots, N]}$ is applied to the noisy data y in order to yield a coarse estimation of the transform-domain signal-dependent noise variance [4]. The deconvolved estimate $\hat{\mathbf{x}}$ can be finally expressed as a function \mathbf{F} of the noisy input signal y as

$$\hat{\mathbf{x}} = \mathbf{F}(y) = \mathbf{R} \Theta \left(\underbrace{\mathbf{D} \mathbf{H}_{\lambda}^{-1} y}_{\mathbf{w}} \right) \underbrace{\tilde{\mathbf{D}} \mathbf{H}_{\lambda}^{-1} y}_{\tilde{\mathbf{w}}} \quad (7)$$

where $\Theta(\mathbf{w}, \tilde{\mathbf{w}}) = [\theta_l(w_l, \tilde{w}_l)]_{l \in [1, \dots, L]}$ represents the pointwise (nonlinear) thresholding function. In this work, we set \tilde{w}_l as the scaling coefficients of the lowpass residual at a given scale l .

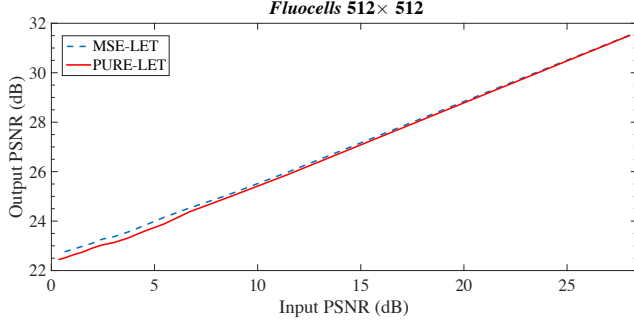


Fig. 2. PSNR comparison of *MSE-LET* and *PURE-LET* for *Fluocells* image where the input PSNR is between 0.37dB ($\alpha = 1400$) and 28.03dB ($\alpha = 1$). The maximum difference between the oracle *MSE-LET* and the proposed *PURE-LET* is 0.27dB.

Corollary 1 Given the transform-domain pointwise processing $\mathbf{F}(\cdot)$ defined by (7), the approximation of the *PURE* estimate $\tilde{\epsilon}$ introduced in (4), can be further expressed as

$$\begin{aligned} \tilde{\epsilon} = & \frac{1}{N} \|\mathbf{F}(\mathbf{y})\|^2 - \frac{2}{N} \mathbf{y}^T \mathbf{H}_\beta^{-T} \mathbf{F}(\mathbf{y}) + \\ & \frac{2\alpha}{N} \left(\partial_w \Theta(\mathbf{w}, \bar{\mathbf{w}})^T [(\mathbf{D}\mathbf{H}_\lambda^{-1}) \bullet (\mathbf{H}_\beta^{-T} \mathbf{R})^T] \mathbf{y} + \right. \\ & \left. \partial_{\bar{\mathbf{w}}} \Theta(\mathbf{w}, \bar{\mathbf{w}})^T [(\bar{\mathbf{D}}\mathbf{H}_\lambda^{-1}) \bullet (\mathbf{H}_\beta^{-T} \mathbf{R})^T] \mathbf{y} \right) \end{aligned}$$

where $\partial_w \Theta(\mathbf{w}, \bar{\mathbf{w}})$ and $\partial_{\bar{\mathbf{w}}} \Theta(\mathbf{w}, \bar{\mathbf{w}})$ represents the first derivative with respect to \mathbf{w} and $\bar{\mathbf{w}}$ of each thresholding function θ_l , respectively. “ \bullet ” denotes the Hadamard product between two matrices.

The whole deconvolution process can be linearly parametrized as

$$\mathbf{F}(\mathbf{y}) = \sum_{m=1}^M \sum_{l=1}^L \sum_{j=1}^J a_{m,l,j} \underbrace{\mathbf{R}_j \theta_l(\mathbf{w}_{m,j}, \bar{\mathbf{w}}_{m,j})}_{\mathbf{F}_{m,j,k}(\mathbf{y})} + \underbrace{\mathbf{R}_{J+1} \mathbf{D} \mathbf{J}_{+1} \mathbf{y}}_{\text{lowpass subband}}$$

where $\mathbf{w} = \mathbf{D}\mathbf{H}_\lambda^{-1} \mathbf{y}$, $\bar{\mathbf{w}} = \bar{\mathbf{D}}\mathbf{H}_\lambda^{-1} \mathbf{y}$, M is the number of Wiener filters (typically $M = 3$), L is the number of elementary pointwise thresholding functions (typically $L = 2$) and J denotes the number of highpass wavelet subbands (typically $J = 12$ for four decomposition levels). In this work, we propose the following *subband-adaptive* thresholding function $\theta_{j,l}$ as:

$$\begin{cases} \theta_{j,1}(w, \bar{w}) = w \left(1 - \exp \left(- \left(\frac{w}{4t_j(\bar{w})} \right)^4 \right) \right) \\ \theta_{j,2}(w, \bar{w}) = w \left(1 - \exp \left(- \left(\frac{w}{9t_j(\bar{w})} \right)^4 \right) \right) \end{cases} \quad (8)$$

where $t_j(\bar{w}) = \sqrt{2^{-j/2} \cdot \tanh(\tau \bar{w}) \bar{w}}$ and τ is empirically set to be 100, so that $x \tanh(\tau x) \approx |x|$. As indicated by (6), we have $K = M \times J \times L$ parameters to determine and they are given by the solution of the linear system of equations (6) of order K .

4. EXPERIMENT AND RESULTS

4.1. Experimental settings

We perform experiments over three images, *Camerman*, *Moon* and *Fluocells*. The original images are firstly convolved by Gaussian kernel with variance 3. The blurred images are subsequently

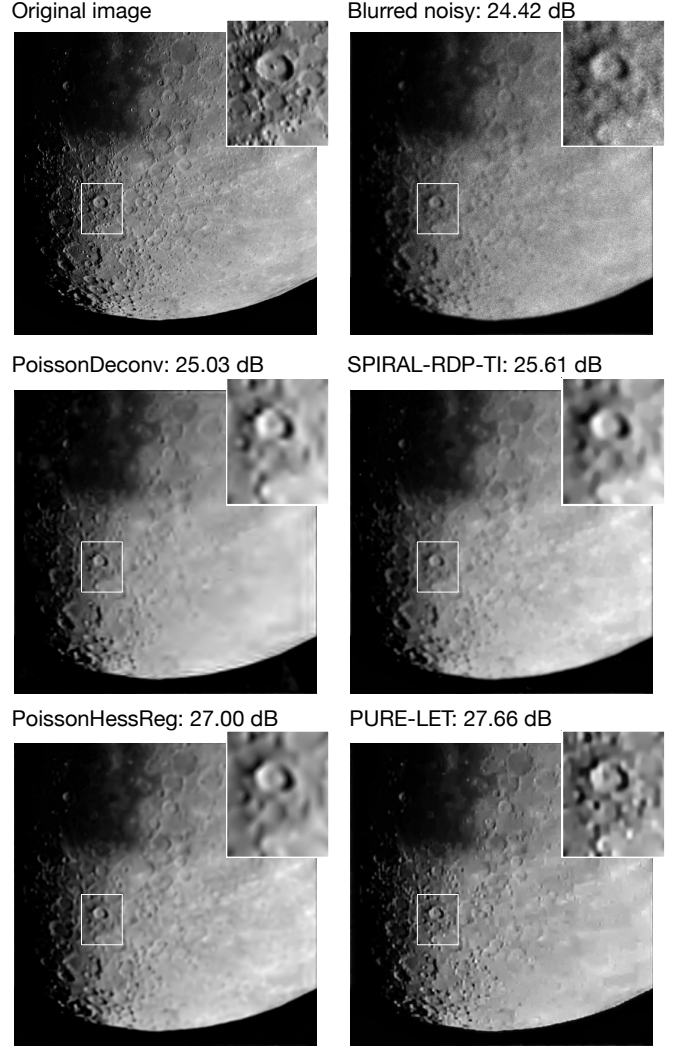


Fig. 3. Restoration of *Moon* image degraded by Gaussian blur and Poisson noise with $\alpha = 1$. The computational time of *PURE-LET* is 6.5s while other approaches need more than 146.3s.

contaminated by Poisson noise with different noise levels (corresponding to different α). The algorithm performance is measured by the peak signal-to-noise ratio (PSNR), defined as $\text{PSNR} = 10 \log_{10}(I_{\max}^2 / (\|\hat{\mathbf{x}} - \mathbf{x}\|^2 / N))$, where I_{\max} is the maximum intensity of the noise-free image. Note that all the reported results have been averaged over 10 noise realizations.

In the proposed method, we use $M = 3$ Wiener filters with $\lambda_1 = 10^{-4} \alpha \mu$, $\lambda_2 = 10^{-3} \alpha \mu$ and $\lambda_3 = 10^{-2} \alpha \mu$, where μ is the expected value of \mathbf{y} . The undecimated Haar wavelet transform is used and the decomposition level is set to be 4 ($J = 12$). Thus we will have $K = 3 \times 2 \times 12 = 72$ coefficients to be determined via solving (6).

4.2. Validation: *PURE-LET* vs *MSE-LET*

To validate the use of the *PURE*, we compare the performance of the *PURE-LET* to the optimal performance achieved when using the *MSE* in the *LET* framework. In other words, the *MSE* is used directly in (6) leading to an oracle solution obtained by the pointwise thresholding proposed in (8) and solving $\mathbf{M}_{\text{aMSE}} = \mathbf{F}^T \mathbf{x}$. This

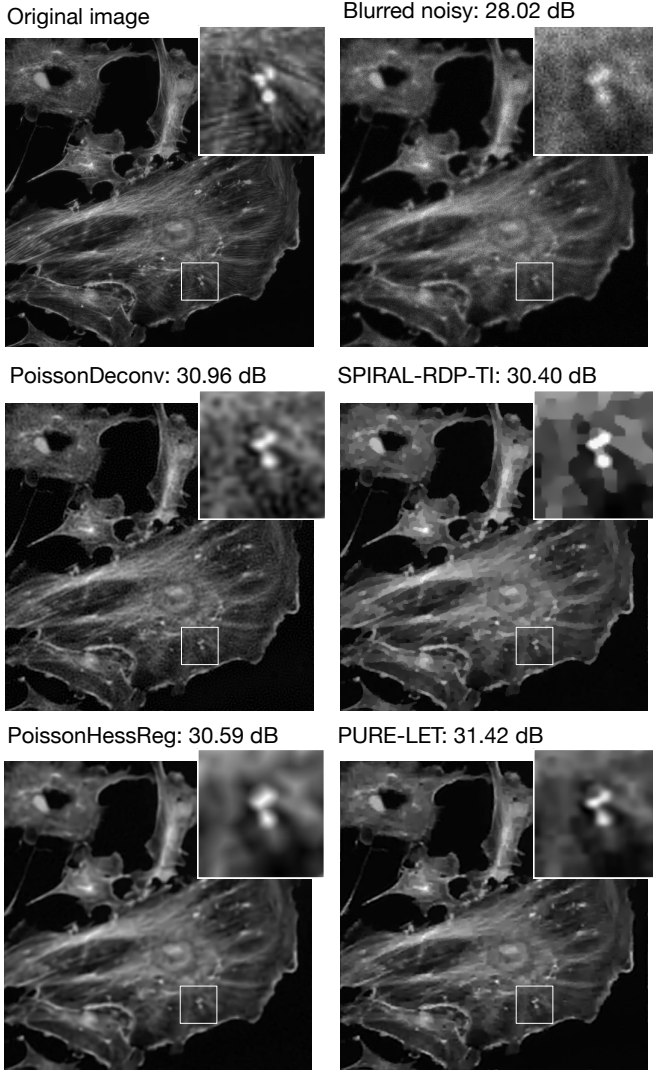


Fig. 4. Restoration of *Fluocells* degraded by Gaussian blur and Poisson noise with $\alpha = 1$. The computational time of PURE-LET is 7.15s while other approaches need more than 124.99s, see Table 2 for details.

oracle solution is named as the *MSE-LET*. The comparison of the PURE-LET and *MSE-LET* for *Fluocells* image is shown in Fig. 2. As expected, our PURE-LET consistently remains within 0.27dB from the *MSE-LET* for a wide range of noise levels, which is an evidence of the robustness of the proposed PURE-LET approach.

4.3. Comparison with the state-of-the-art

As benchmarks for comparisons, we evaluate our algorithm against three competitive deconvolution techniques specifically designed for Poisson noisy images: *PoissonDeconv* [26], *SPIRAL-TAP-TI* [23] and *PoissonHessReg* [27]. For each of these methods, we used the parameters suggested in their respective publications and softwares.

Table 1 reports the PSNR results we have obtained for the various deconvolution methods over six representative noise levels from $\alpha = 1$ to $\alpha = 200$. This table demonstrates that the PURE-LET consistently outperforms other approaches. We would also like to stress that our algorithm is very robust to a wide range of noise levels. In particular, significant improvements are observed at large α ,

Table 1. PSNR Comparison with some state-of-the-art algorithms under Gaussian blur with variance 3.

α	1	5	10	50	100	200
Image	<i>Cameraman</i> 256×256					
Input	21.59	18.41	16.24	10.07	7.16	4.20
PoissonDeconv	22.78	22.07	21.57	18.65	15.03	10.86
SPIRAL-TAP-TI	24.06	23.12	22.22	20.91	20.30	18.26
PoissonHessReg	23.04	21.97	21.38	19.64	18.70	17.57
PURE-LET	24.46	23.35	22.85	21.41	20.65	19.87
Image	<i>Moon</i> 512×512					
Input	24.42	20.09	17.56	10.99	8.05	5.06
PoissonDeconv	25.03	24.77	24.62	20.66	15.28	11.95
SPIRAL-TAP-TI	25.61	24.15	24.93	22.01	21.68	19.11
PoissonHessReg	27.00	25.73	25.15	23.87	23.27	22.46
PURE-LET	27.66	26.26	25.69	24.35	23.91	23.45
Image	<i>Fluocells</i> 512×512					
Input	28.02	23.57	21.01	14.43	11.46	8.48
PoissonDeconv	30.96	27.75	27.19	21.86	18.51	15.90
SPIRAL-TAP-TI	30.46	28.59	28.05	26.39	25.17	23.18
PoissonHessReg	30.59	28.58	27.60	25.14	24.06	23.17
PURE-LET	31.42	29.69	28.88	26.79	25.81	24.81

* The results have been averaged over 10 noise realizations.

Table 2. Comparison of the computational time of various deconvolution algorithms (Units: seconds).

Degradation scenario	<i>Cameraman</i> 256×256	<i>Fluocells</i> 512×512
	$\alpha = 100$	$\alpha = 10$
PoissonDeconv	210.30	978.84
SPIRAL-TAP-TI	101.61	301.01
PoissonHessReg	22.26	124.99
PURE-LET	1.04	7.15

where the signal-dependent nature of the Poisson noise is more pronounced. Fig. 3 and Fig. 4 show the comparison of visual quality of *Moon* and *Fluocells*, respectively. It is observed that the proposed method preserves various image details, while introducing very few artifacts.

4.4. Computational time

All experiments are carried out on a PC with a 3.3 GHz Intel Core i3, with 4 GB of RAM. Table 2 reports the computational time of various deconvolution algorithms. It can be seen that our method is substantially faster than other approaches. As observed, the proposed PURE-LET algorithm is roughly 22 times faster than the next fastest algorithm for a 256×256 image and 16 times faster for a 512×512 image. It is worth mentioning that the proposed method is implemented using unoptimized MATLAB code only, without any compiled routines.

5. CONCLUSIONS

We proposed a new non-iterative deconvolution approach for Poisson noisy images. We linearly parametrize the deconvolution process as a combination of elementary functions (LET). Each elementary function consists of a Wiener filtering followed by transform-domain thresholding. We then use the purely data-driven unbiased estimate of the MSE (PURE) to optimize these LETs. The proposed PURE-LET approach outperforms current state-of-the-art techniques, both qualitatively and computationally. Moreover, the flexibility and low computational cost of the proposed approach offers a framework for developing more sophisticated algorithms. For example, other transforms such as the block discrete cosine transform and the combination with the discrete wavelet transform, could be employed or multivariate thresholding functions considered.

6. REFERENCES

- [1] L. A. Shepp and Y. Vardi, "Maximum likelihood reconstruction for emission tomography," *IEEE Trans. Med. Imag.*, vol. 1, no. 2, pp. 113–122, 1982.
- [2] P. Sarder and A. Nehorai, "Deconvolution methods for 3-D fluorescence microscopy images," *IEEE Signal Process. Mag.*, vol. 23, no. 3, pp. 32–45, May 2006.
- [3] R. M. Willett and R. D. Nowak, "Platelets: a multiscale approach for recovering edges and surfaces in photon-limited medical imaging," *IEEE Trans. Med. Imag.*, vol. 22, no. 3, pp. 332–350, 2003.
- [4] F. Luisier, T. Blu, and M. Unser, "Image denoising in mixed Poisson-Gaussian noise," *IEEE Trans. Image Process.*, vol. 20, no. 3, pp. 696–708, Feb. 2011.
- [5] J. Schmitt, J.-L. Starck, J.-M. Casandjian, J. Fadili, and I. Grenier, "Multichannel poisson denoising and deconvolution on the sphere: application to the fermi gamma-ray space telescope," *Astron. Astrophys.*, vol. 546, p. A114, 2012.
- [6] R. Neelamani, H. Choi, and R. Baraniuk, "ForWaRD: Fourier-wavelet regularized deconvolution for ill-conditioned systems," *IEEE Trans. Signal Process.*, vol. 52, no. 2, pp. 418–433, 2004.
- [7] K. Dabov, A. Foi, V. Katkovnik, and K. Egiazarian, "Image restoration by sparse 3d transform-domain collaborative filtering," *Proc. SPIE Electron. Imag.*, vol. 6812, pp. 701–712, 2008.
- [8] H. Takeda, S. Farsiu, and P. Milanfar, "Deblurring using regularized locally adaptive kernel regression," *IEEE Trans. Image Process.*, vol. 17, no. 4, pp. 550–563, 2008.
- [9] J. Guerrero-Colón, L. Mancera, J. Portilla *et al.*, "Image restoration using space-variant gaussian scale mixtures in over-complete pyramids," *IEEE Trans. Image Process.*, vol. 17, no. 1, pp. 27–41, 2008.
- [10] F. Xue, F. Luisier, and T. Blu, "Multi-Wiener SURE-LET deconvolution," *IEEE Trans. Image Process.*, vol. 22, no. 5, pp. 1954–1968, Mar. 2013.
- [11] W. H. Richardson, "Bayesian-based iterative method of image restoration," *J. Opt. Soc. Am. A*, vol. 62, no. 1, pp. 55–59, 1972.
- [12] L. B. Lucy, "An iterative technique for the rectification of observed distributions," *The Astron. J.*, vol. 79, p. 745, 1974.
- [13] N. Dey, L. Blanc-Feraud, C. Zimmer, P. Roux, Z. Kam, J.-C. Olivo-Marin, and J. Zerubia, "Richardson-lucy algorithm with total variation regularization for 3d confocal microscope deconvolution," *Microsc. Res. Tech.*, vol. 69, no. 4, pp. 260–266, 2006.
- [14] R. M. Willett, Z. T. Harmany, and R. F. Marcia, "Poisson image reconstruction with total variation regularization," in *Proc. IEEE Int. Conf. Img. Proc.*, 2010, pp. 4177–4180.
- [15] J.-L. Starck, F. Murtagii, and A. Bijaoui, "Multiresolution support applied to image filtering and restoration," *Graph. Model. Im. Proc.*, vol. 57, no. 5, pp. 420–431, 1995.
- [16] M. Carlván and L. Blanc-Feraud, "Sparse Poisson noisy image deblurring," *IEEE Trans. Image Process.*, vol. 21, no. 4, pp. 1834–1846, Mar. 2012.
- [17] M. Bertero, P. Boccacci, G. Desiderà, and G. Vicidomini, "Image deblurring with Poisson data: from cells to galaxies," *Inverse Probl.*, vol. 25, no. 12, pp. 123 006–27, Nov. 2009.
- [18] A. Danielyan, V. Katkovnik, and K. Egiazarian, "Deblurring of poissonian images using bm3d frames," in *Proc. SPIE 8138, Wavelets and Sparsity XIV*, 2011, pp. 8 138 121–7.
- [19] L. Ma, L. Moisan, J. Yu, and T. Zeng, "A dictionary learning approach for Poisson image deblurring," *IEEE Trans. Med. Imag.*, vol. 32, no. 7, pp. 1277–1289, Jul. 2013.
- [20] M. A. Figueiredo and J. M. Bioucas-Dias, "Restoration of poissonian images using alternating direction optimization," *IEEE Trans. Image Process.*, vol. 19, no. 12, pp. 3133–3145, 2010.
- [21] P. Fryzlewicz and G. P. Nason, "A Haar-Fisz algorithm for poisson intensity estimation," *J. Comput. Graph. Stat.*, vol. 13, no. 3, pp. 621–638, 2004.
- [22] R. Willett, "Multiscale analysis of photon-limited astronomical images," in *Statistical Challenges in Modern Astronomy IV*, vol. 371, 2007, pp. 247–264.
- [23] Z. T. Harmany, R. F. Marcia, and R. M. Willett, "This is SPIRAL-TAP: Sparse Poisson Intensity Reconstruction ALgorithms–Theory and Practice," *IEEE Trans. Image Process.*, vol. 21, no. 3, pp. 1084–1096, Feb. 2012.
- [24] T. Blu and F. Luisier, "The SURE-LET approach to image denoising," *IEEE Trans. Image Process.*, vol. 16, no. 11, pp. 2778–2786, 2007.
- [25] M. Raphan and E. P. Simoncelli, "Optimal denoising in redundant representations," *IEEE Trans. Image Process.*, vol. 17, no. 8, pp. 1342–1352, 2008.
- [26] F. X. Dupé, J. M. Fadili, and J. L. Starck, "A proximal iteration for deconvolving Poisson noisy images using sparse representations," *IEEE Trans. Image Process.*, vol. 18, no. 2, pp. 310–321, Mar. 2009.
- [27] S. Lefkimmiatis and M. Unser, "Poisson image reconstruction With Hessian Schatten-Norm regularization," *IEEE Trans. Image Process.*, vol. 22, no. 11, pp. 4314–4327, Sep. 2013.